Measurement of the plasma edge profiles using the combined probe on W7-X

P. Drews[1], Y. Liang[1], S. Liu[1], A. Krämer-Flecken[1], O. Neubauer[1], J. Geiger[2], M. Rack[1], D. Nicolai[1], O.Grulke[2], C. Killer[2], N. Wang[3], A. Charl[1], B. Schweer[1], P. Denner[1], M. Henkel[1], Y. Gao[1], K. Hollfeld[4], G. Satheeswaran[1], N. Sandri[1], D. Höschen[1] and the W7-X Team[2]

[1]Forschungszentrum Jülich GmbH, Institut fur Energie- und Klimaforschung Plasmaphysik, Partner of the Trilateral Euregio Cluster (TEC), 52425 Jülich, Germany
[2]Max-Planck-Institut für Plasmaphysik, Greifswald, Germany
[3]School of Electrical and Electronic Engineering, Huazhong University of Science and Technology, Wuhan 430074, China
[4]Forschungszentrum Jülich GmbH, Central Institute for Engineering, Electronics and Analytics/Engineering and Technology (ZEA-1), 52425 Jülich, Germany

Corresponding Author: p.drews@fz-juelich.de

Abstract:

Wendelstein 7-X (W7-X), started operation in December 2015 with a limiter configuration. In conjunction with the multi-purpose manipulator, a carrier for fast reciprocating probe systems, the combined probe has been installed. This combined probe is able to measure the local electron temperatures and densities, magnetic field, the electric field and the plasma flow. These parameters are very useful in ascertaining the edge plasma perfomance. In addition, the field line tracing feature of the W7-X webservices was used to calculate the connection length along the path of the probe, for each configuration.

1 Introduction

Wendelstein 7-X (W7-X), one of the worlds largest optimized stellarators, located at the IPP Greifswald, started operation recently with a limiter configuration [1]. Both, helium and hydrogen plasmas were used as working gases, with discharge durations of up to 6 s and 4 MJ of maximum heating input energy from the electron cyclotron resonance heating (ECRH). Edge plasma profile measurements, especially those of the electron temperature and density, will play a key role in validating the performance in comparison to the tokamak and hence the viability of a stellarator fusion reactor. The up-stream measurements of the temperature and density conducted with the combined probe, complement those down-stream on the limiters and also serve as input parameters for the EMC3-EIRENE transport modelling [2]. Part of this first campaign were studies of the configuration

effects of the magnetic topology on the transport. It was a stated aim [3] to find a configuration that has a optimized neoclassical transport and also the powerloads on the limiter or divertor for future long pulse operation have to be optimized. The combined probe was employed together with the multi-purpose manipulator to obtain the plasma edge profiles. It consists of an array of two 3D magnetic pick up coils, a Mach probe and a set of five Langmuir pins, with three of them being used in a triple probe configuration. This paper describes the measurements conducted with the combinded probe, section 1.1 will give details about the diagnostic, section 2 shows the measurements using the combined probe and section 2.1 discusses the iota dependency of the 5/5 island positions, the pressure and density decay length. It should be noted that limiter configuration was chosen to supress the formation of egde islands, for the highest iota configuration the 5/5 island is not shadowed by the limiters and visible in the Langmuir probes profiles. The pressure decay length calculated with the electron density and temperature profiles is greatly important to determine the handling of the heatloads on the limiters. In comparison with other experiments it is shown that the measured decay lengths are of similar magnitude or even bigger. These measurements also serve to confirm the modelled magnetic configuration by directly measuring the local magnetic field and confirming the existence and position of edge islands.

1.1 Experimental setup

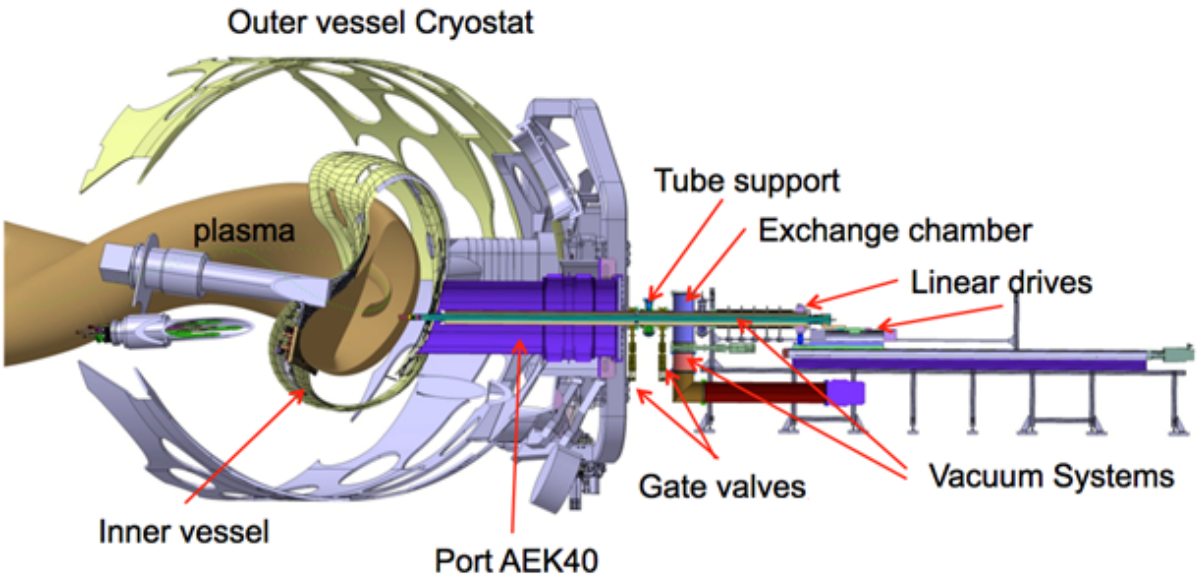

FIG. 1: Sketch of the Multi-purpose manipulator (MPM) installed on W7-X

The multi-purpose manipulator (MPM), shown in figure 1, was installed at the low field side of the vacuum vessel on W7-X in 2015 and commissioned in early February 2016 [4][5], in order to mount a wide variety of diagnostic probes for measurements of the plasma

edge parameters and for plasma wall interaction studies, the manipulator allows both measurements in a static position to observe fluctuation and a fast movement for obtaining profiles. It is located in the midplane of module four at the so-called AEK40 flange at the toroidal position ($\phi = 200.7°$) and able to plunge 35 cm into the vacuum vessel. The maximum acceleration was set to 30 $\frac{\mathrm{m}}{\mathrm{s}^2}$ and a maximum velocity of 3.5 $\frac{\mathrm{m}}{\mathrm{s}}$. The maximum plunge depth of the manipulator that was used during the first operational phase (Op. 1.1) was 30 cm, with an duration of approximately 250 ms. The first diagnostic to be used was the so-called combined probe, the combined probe includes two 3D magnetic pick-up coil arrays (similar to those in [6]), five Langmuir probe pins [7], and a Mach setup [8]. This allowed to simultanously measure the edge radial profiles of the magnetic fields, the electron temperature and density, the electric field and the plasma flow. The Langmuir and Mach probes are located on the top facing of the combined probe, the probe pins are insulated from the conducting cover by aluminum-oxide ceramics. The Langmuir probe array consists of three floating potential pins, that deliberately differ in radial and poloidal position, for the calculation of the electric field and correlation of the radially and poloidally separated floating potential measurements. In addition, one pin is negatively biased in order to measure the ion saturation current I_{sat} and another pin is positively biased with voltage U_+ to collect electrons. A set of four capacitors was used to supply biasing voltages of up to 160 V with a capacitance of 5.8 F, thus for each biased pin a single power supply was available. For the experiment a biasing of 150 V was used.

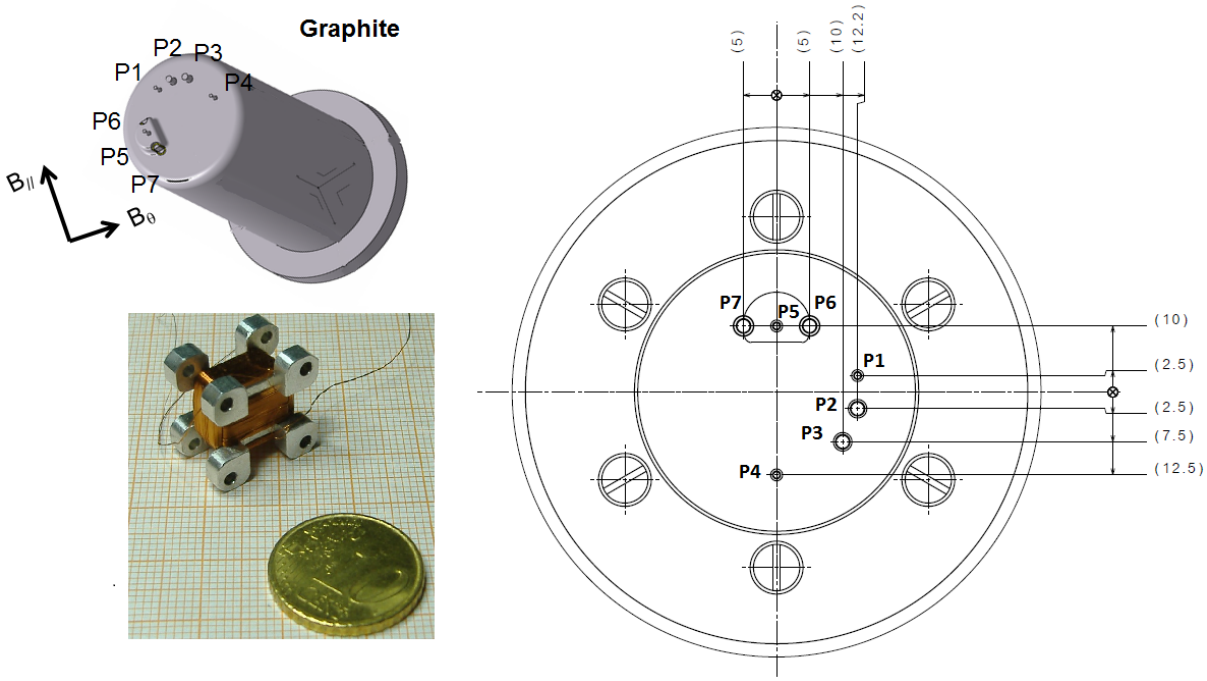

FIG. 2: Left top: Sketch of the combined probe with graphite cover, left bottom: 3D pick-up coil, right: Arrangement of the Langmuir pins with distances in mm

The Langmuir probe measurements yielded temperature, density and electric field

profiles, in addition also time traces for the temperature and density and the plasma edge, with the MPM in fixed position, were recorded. The Langmuir probe shown in figure 2 contains three floating potential pins (P1, P4, P5), with pin P5 being on a stage 3 mm radialy deeper. The distance of the pins to each other is about ≈ 5 mm, which is considerably larger then the Debye length of about $\lambda_D \approx 3 \cdot 10^{-2}$ mm. This arrangement of the floating potential pins was made to allow turbulence studies via correlating the differently radially and poloidally placed probes. In addition two pins (P6 and P7) were located in parallel to the toroidal magnetic field direction, separated by the stage on the probe surface, biased negatively and used as a Mach probe. For the material for both Langmuir and Mach probe pins tungsten was chosen for its resistance to heat loads. The pick-up coils, shown in figure 2 on the right, are arrayed as a set of two 3D coils wound around each other, the coils diameter is about 1 cm. Their area is about 1.5 cm^2 for the outermost coil and 1.15 cm^2 for inner one, with $n = 300$ windings. They are radially seperated by about 3.2 cm along the probe and the upper one is 2.4 cm away from the top cover of the probe. All experimental data was sampled at 1 MHz, the signal conditioners for the Langmuir probe measurements operated to a maximum of 300 kHz and the pick-up coils up to 200 kHz. The lower frequency range was selected for the pick-up coils since the graphite shielding attenuates signals beyond 60 kHz strongly. The experimental data presented here was filtered using a lowpass Butterworth filter with a cut-off frequency of 0.1 kHz.

2 Measurements

The combined probe was used to measure the electron temperature and density, the magnetic field profiles and the electric field outside of the last closed flux surface. The iota configuration was changed by tuning the planar and non-planar coil currents according to table I. The measurements were performed at the same ECRH heating of 2 MW. The higher iota configurations experience an inwards shift of the 5/6 island chain located inside the last closed flux surface, while the 5/5 island moves closer towards the last closed flux surface from the scrape off layer. It is not possible for the probe to measure the 5/6 island chain directly and the 5/5 island chain is supposed to be cut off by the limiter. The Poincaré plots for the index 1, 7 and 13 configurations of the iota scan in the toroidal section of the manipulator are shown in figures 3, 4 and 5. The machine performance had considerably improved with the conditioning, such that the line averaged densities were consistent throughout the day. It was assumed that $T_e = T_i$ for the calculation of electron density, since for the first campaign no diagnostic was operational that could measure the ion temperature with the same resolution at the edge as the Langmuir probes did for the electrons. The calculation of the electron density also depends on sufficient knowledge of the ion species and their charge state:

$$n_e = \frac{I_{sat}}{0.49\, A_{eff} \sqrt{\frac{T_i + Z\, T_e}{m_i}}}, \tag{1}$$

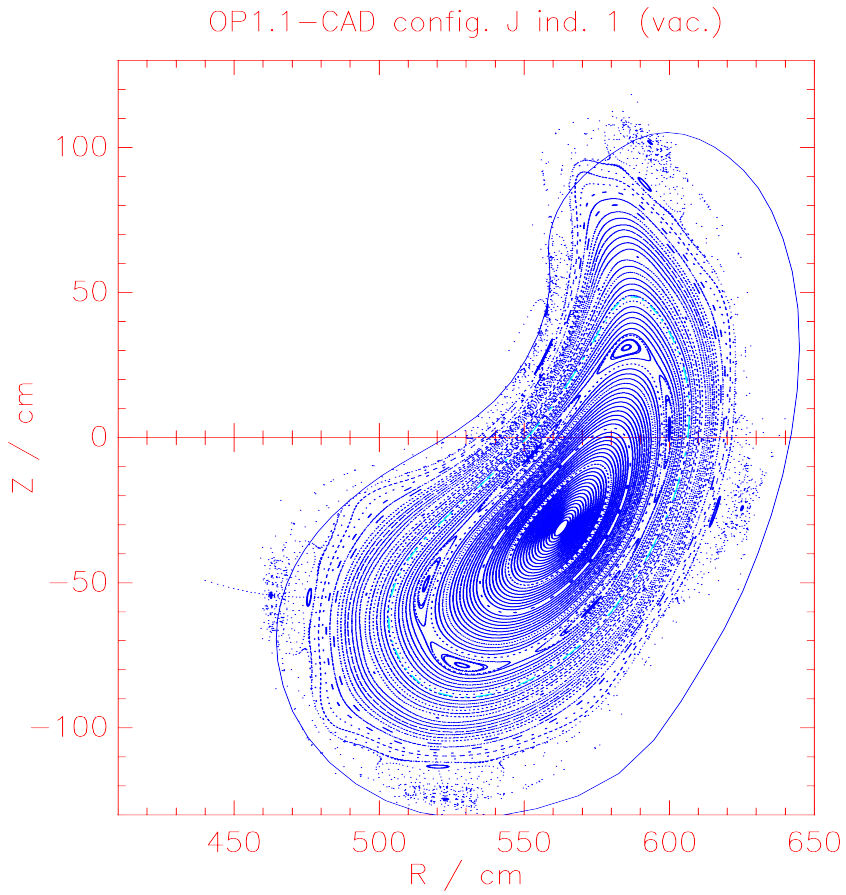

FIG. 3: Poincaré plot for the index 1 configuration of the iota scan in the toroidal section of the manipulator, indicated in light blue is the last closed flux surface

With A_{eff} as the effective collection area. Due the huge difference in gradient scale length $L \approx 2\,\text{m}$ of the magnetic field and the Lamor radius of both electrons $r_{\text{Le}} \approx 0.44 \cdot 10^{-5}\,\text{m}$ and ions $r_{\text{Li}} \approx 0.19 \cdot 10^{-3}\,\text{m}$ the sheath expansion coefficient 0.49 for plasmas in strong magnetic fields [9] was used. The effective charge is estimated to be between $Z = 2 - 6$, which clearly indicates that the plasma considered here is not a pure hydrogen plasma, with the main impurity source in this case carbon originating from the limiters. Given the above effective charge a maximum of 10 % carbon content is a good estimate. Until now no precise measurements on the impurity concentration and effective charge have been made at the edge and the above mentioned conditions serve as another possible source of error in the density measurements. The errors presented here were calculated by using the weighted standard deviation of the data. The density has a comparably large error due to the small currents measured via a shunt resistor. The measurements of the electron temperature were compared to the limiter Langmuir probes [10]. The manipulator mounted combined probe is measuring upstream values of up to a maximum of 25 eV. While the limiter Langmuir probes yield downstream values of between 15 eV and 50 eV [11]. It was shown in [11] that the set of limiter Langmuir probes while being

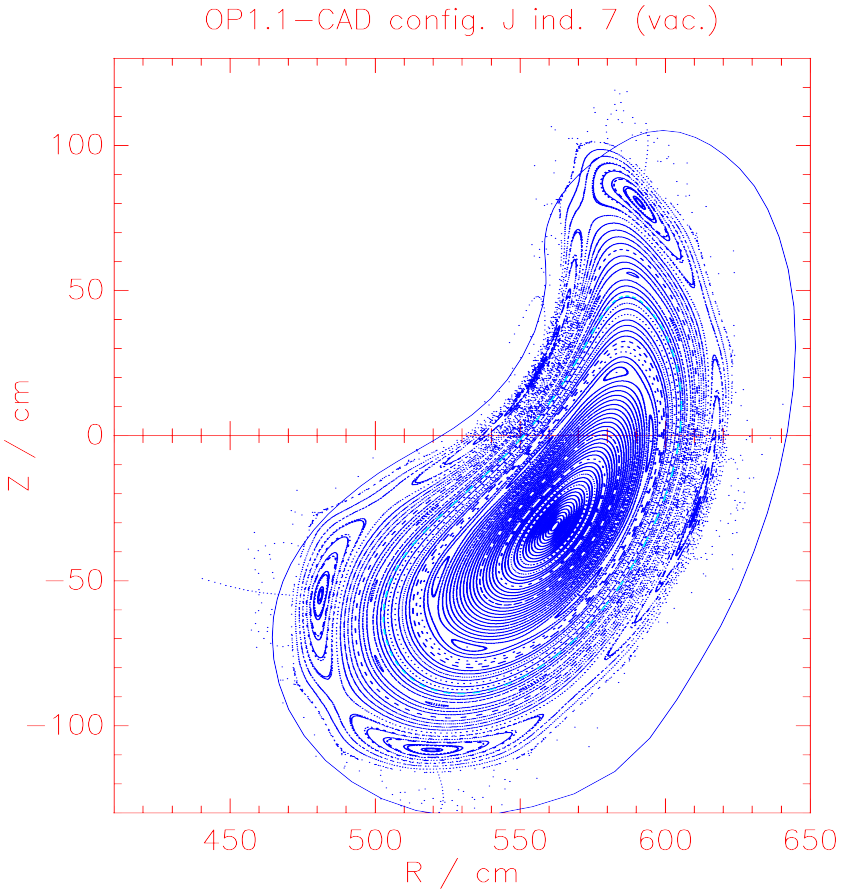

FIG. 4: Poincaré plot for the index 7 configuration of the iota scan in the toroidal section of the manipulator, indicated in light blue is the last closed flux surface

more close to the last closed flux surface and thereby yielding higher temperatures, had a very similar exponential decay compared to the profiles measured with the combined probe.

The Max-Planck-Institut für Plasmaphysik in Greifwald offers a webservice based field line tracing tool [12], the tool traces the field lines for given input currents and machine configurations by integrating the equation:

$$\frac{\mathrm{d}\vec{r}(s)}{\mathrm{d}s} = \frac{\vec{B}}{|\vec{B}|} \tag{2}$$

Considered here were the Op. 1.1 limiter configurations listed in table I, the field line tracing tool was used to identify the confined region, by assuming that it is marked by consistently exceeding a connection length of 300 m as shown in figure 8. The pick up coils were used to measure the magnetic field profiles, the direct comparison of the calculation from the field line tracing webservice and the measurement is difficult due to the pick up

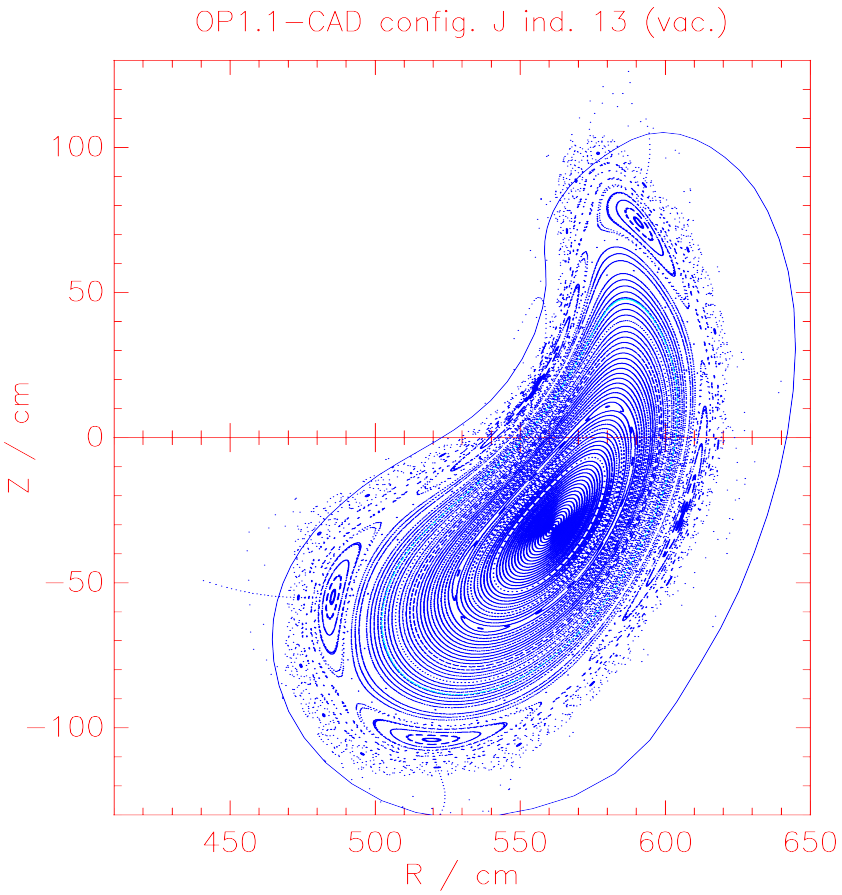

FIG. 5: Poincaré plot for the index 13 configuration of the iota scan in the toroidal section of the manipulator, indicated in light blue is the last closed flux surface

coils detecting the temporal change:

$$\dot{B} = -ANU_{\text{induced}} \tag{3}$$

with A as the pick-up coil area, N the number of coil windings and U_{induced} the induced voltage. After integrating the resulting $\dot{B}$ one can caculate the gradient in radial direction which is independent of any integration constants. Figure 7 shows the profile of the magnetic field gradients for the two pick up coils and the calculated values, the expected magnetic field values match those of the measurements.

2.1 Iota-scan experiment

It is clearly visible in the density and temperature profiles (see figure 6), that the magnetic axis and therefore also the last closed flux surface (LCFS) was shifted. The connection length for the chosen scenarios shown in figure 8 indicate a similar shift of the profiles. The 2D plots of the magnetic topology in a toroidal cross-section for the J-configuration index 1, index 7, index 9 and index 13 at the position of the manipulator show a strong change

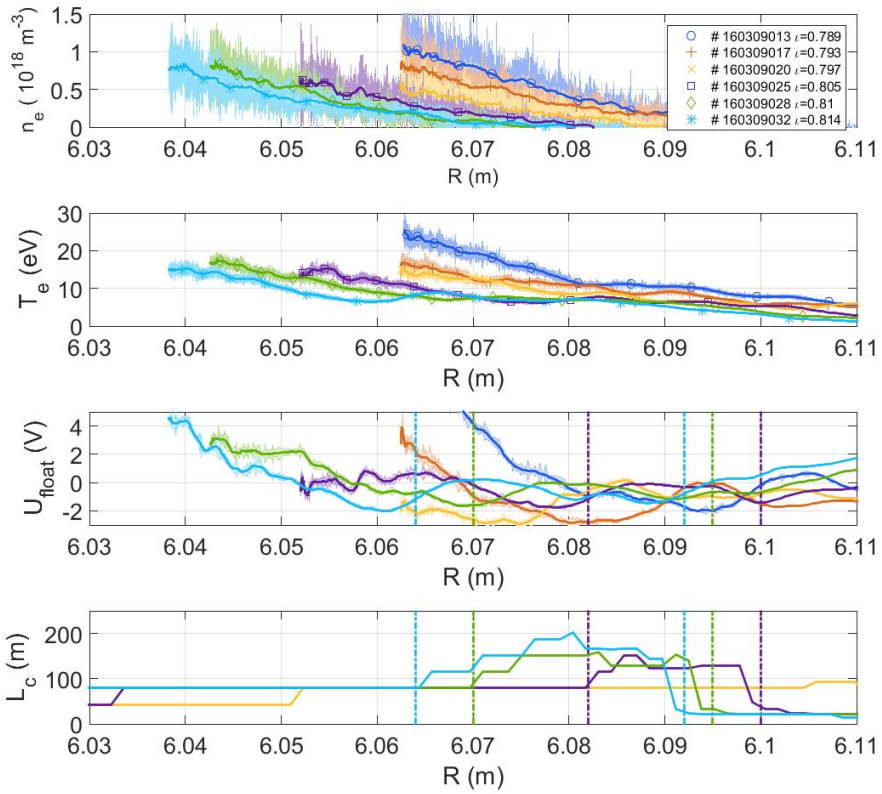

FIG. 6: Temperature, density, plasma potential and connection length profiles of the iota scan. The vertical lines in the plasma potential and connection length plot profile indicate the location of the high connection length areas in front of the last closed flux surface

of the connection length in the plasma edge. The W7-X field line tracing webservice was used to calculate the connection length along the path of the combined probe. The connection length calculations show that with increasing iota a region of high connection appears a few cm in front of the least closed flux surface. In figure 8 one can see for increasing configuration the largest region of high connection length before the actual last closed surface increase with higher iota, this is due to the 5/5 islands moving away from limiters. The Poincaré plots in the figures 3, 4 and 5 predict such a shift of the islands. For the iota index 13 configuration this effect is visible in the temperature profile in figure 6, which is well correlated with the high connection length region in the plot below. For the lower configurations this effect is at best barely visible in the temperature and density profiles. But taking a look at the plasma potential one can see that those regions cause a local peaking in the profile matching the position of the high connection length regions, similar behavior of the plasma potential is also visible for the index 11 and 9 configurations. Such observations have been made at the helically symmetric experiment

TABLE I: Coil configurations considered for the iota scan, with the position of the last closed flux surface (LCFS) in the path of the manipulator, obtained from the field line tracing and central iota value

Scenario#	**Index**	**Position of LCFS (m)**	**iota**
20160309.013	1	6.03	0.789
20160309.017	5	6.025	0.793
20160309.020	7	6.016	0.797
20160309.025	9	6.01	0.805
20160309.028	11	6.004	0.81
20160309.032	13	6.001	0.814

(HSX) [13]and at the Large Helical Device (LHD) [14], with the notable difference that the LHD contains a more complex structure of remnant magnetic islands, stochastic fields and edge surface layers. The density decay length λ_{n_e} was obtained from:

$$n_e(r) = n_0 \exp\left(\frac{r - R_0}{\lambda_{n_e}}\right). \tag{4}$$

The electron pressure is calculated using the temperature and density profiles, by multiplying n_e and T_e. From this electron pressure profile the power decay length λ is deduced by fitting the function below to the data:

$$p_e(r) = p_0 \exp\left(\frac{r - R_0}{\lambda_{p_e}}\right). \tag{5}$$

For R_0 the values of the position of the last closed flux surface calculated by the field line tracing tool were used. Figure 9 shows the pressure profiles and the fitted functions, this pressure decay length is recognized as a crucial quantity concerning peak heat loads [15]. On the right hand side the power decay length and electron density decay length against the central iota value is plotted. The decay lengths were obtained from the fit of the data and the error is calculated by fitting the same exponential functions to the two most extreme cases of the upper and lower error bound. The values from obtained from the experiment do not show that the pressure decay length changes considerably with increasing iota. This rather broad decay length for W7-X is larger than the ones found for Tokamaks of comparable size, indeed the pressure decay lengths reported for ASDEX Upgrade are at about 5 mm [16], for other tokamaks decay lengths of the same magnitude are found in [17]. It also quite well matches the prediction from field line diffusion modelling with 1.5 cm [18]. Additionally the calculated density decay lengths are similar to the decay lengths of the particle flux, which is mostly a function of the density, found at W7-AS [19] and about 1 cm at LHD [20]. It should be mentioned at this point that the comparisons were taken from machines with a divertor configuration. These findings have to be compared to the measured heat loads on the limiter (see [11] and [21]).

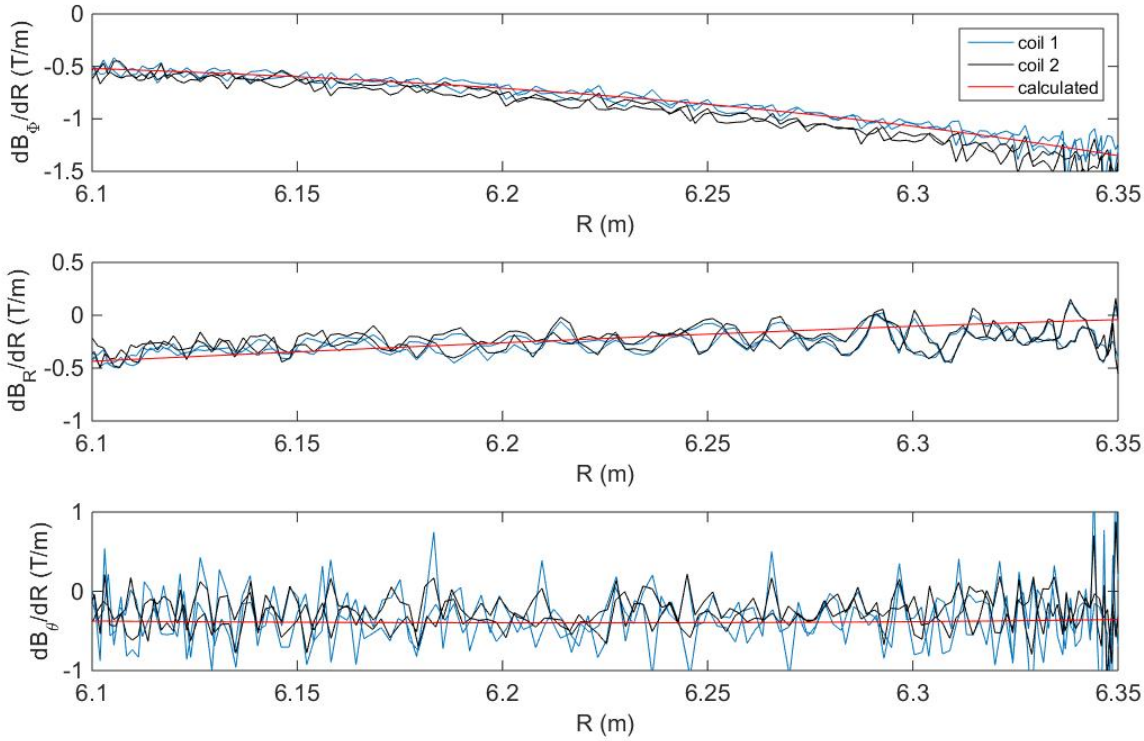

FIG. 7: Magnetic field gradients in radial direction measured with the two pick up coil arrays in comparison to the calculation from the field line tracing webservice

2.2 Measurement of the electric field E_r

The electric field was measured using the floating potential pins which were $\Delta R = 3\,\mathrm{mm}$ radially apart. The electric field is calculated using:

$$E_\mathrm{r} = -\frac{\partial(U_\mathrm{float} + 2.8 \cdot T_\mathrm{e})}{\partial r} = -\left(\frac{U_\mathrm{float-up} - U_\mathrm{float-down}}{\Delta R} + 2.8\frac{T_\mathrm{e}(r+\Delta r) - T_\mathrm{e}(r)}{\Delta r}\right). \quad (6)$$

It is necessary here to take the $T_\mathrm{e}(r)$ from the profile, since there are not two independent temperature measurements in different radial positions. The selection using a low pass filter with a cut-off frequency of 50 Hz was necessary to obtain the data. The values of the electric field from the combined probe close to its final position are prone to error as the $1/\Delta r$ term becomes very large. The measurements of the electric field can be compared to those of the reflectometry [22]. It is expected that the sign of the electric field changes from positive to negative while crossing the last closed flux surface at $r_\mathrm{eff}/a = 1$. While measurements done with the Langmuir probes yield mostly positive values as expected from its position in front of the last closed flux surface. Therefore, the last closed flux surface is located further inwards relative to the probe position. This

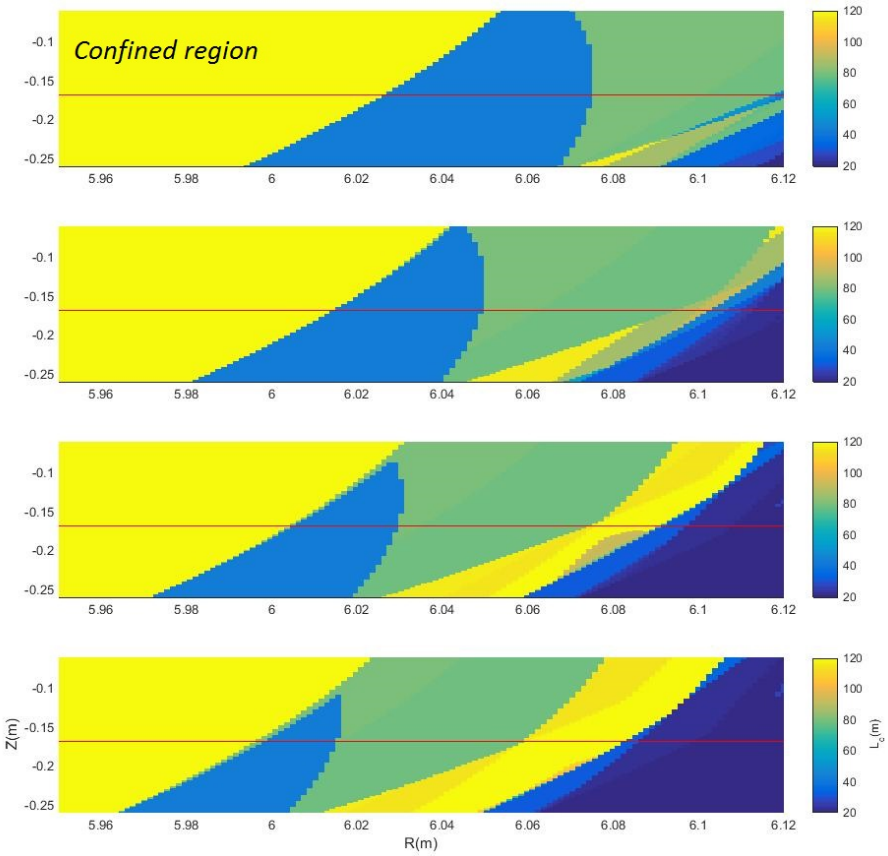

FIG. 8: Connection length calculated for the iota scan, J configuration index 1, index 7 configuration, index 9 configuration, index 13 configuration, the red line indicates the path of the manipulator

is further supported by the aforementioned relatively low values from the density and temperature measurements. For the next operational phase plunges reaching to densities of at least $0.6 \times 10^{19}\,\mathrm{m}^{-3}$ are necessary to obtain a matching range of both reflectometry and combined probe.

3 Summary and Outlook

The combined probe measured the edge plasma profiles of the electron temperature, density, electrical field and magnetic field. The measurements of the Langmuir probe mounted on the manipulator is in agreement with the limiter Langmuir probes, if ones takes the more outward position of the manipulator probe into account. The measured magnetic profiles yield a good agreement with the values expected from calculations. The

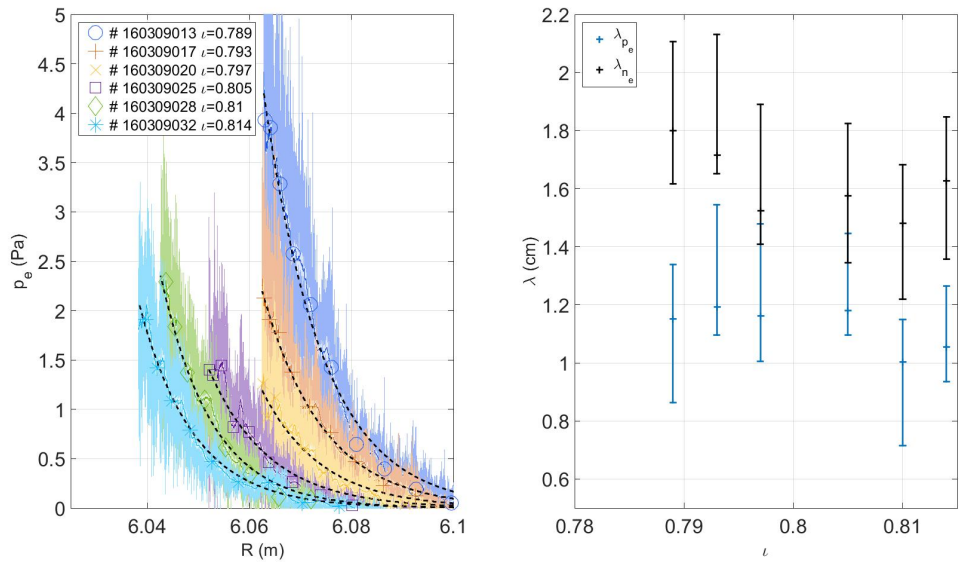

FIG. 9: Left: pressure profiles of the iota scan, right: pressure and density decay length obtained from fit versus central iota

profiles of the floating potential and the temperature were able to confirm the position and extend of the 5/5 for the highest iota configuration. It was shown that pressure decay lengths do not change with the iota configuration and that they agree well with the expected decay length from the modelling. The decay lengths are comparable to those found in other machines or even bigger, which is promising for the future exploitation of the experiment with more heating power and longer discharges. The measurements of the electric field using the combined probe yield positive values is in agreement with the probe's position outside of the last closed flux surface. The existing probe will be improved upon concerning the arrangement of the floating potential pins for correlation measurements, the Mach probe pins will have their ceramic insulator on the plasma facing side removed, to prevent any possible leak currents and an ion sensitive probe for simultaneous measurements of the ion temperature is being prepared. It is planned, in the second operational phase, to use the combined probe together with the DIAS camera system [23], a retarding field analyzer probe, a mach probe and a dedicated probe for fluctuation measurements in conjunction with modelling [24].

References

[1] DINKLAGE A. et al., Confinement in Wendelstein 7-X Limiter Plasmas, Proceedings of the 43nd EPS (2016)

[2] RACK, M. et al., A fluidkinetic approach for 3D plasma edge transport in He-plasma, Nucl. Fusion **57** (2017) 056011

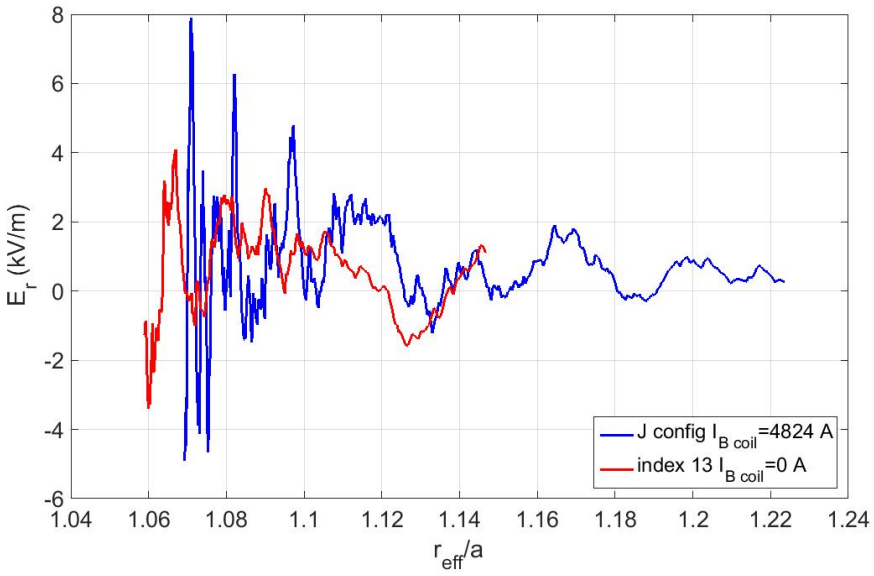

FIG. 10: Electric field measured with the combined probe for the J and high iota configuration

[3] KLINGER T. et al., Performance and properties of the first plasmas of Wendelstein 7-X, Plasma Phys. Control. Fusion **59** (2017) 014018

[4] NICOLAI D. et al., A Multi-Purpose Manipulator system for W7-X as user facility for plasma edge investigation, Fusion Eng. Des. (2017), http://dx.doi.org/10.1016/j.fusengdes.2017.03.013

[5] SATHEESWARAN G. et al., A PCS7 -based control and safety system for operation of the W7-X Multi-Purpose Manipulator facility, Fusion Eng. Des. (2017), https://doi.org/10.1016/j.fusengdes.2017.05.125

[6] YANG Y. et al., Experimental observations of plasma edge magnetic field response to resonant magnetic perturbation on the TEXTOR Tokamak Nucl. Fusion **52** (2012) 074014

[7] TONKS and LANGMUIR, A General Theory of the Plasma of an Arc Phys Rev. **34** (1929) 876-922

[8] CHUNG K. et al.,Mach probes, Plasma Sources Sci. Technol. **21** (2012) 063001

[9] THOMPSON W. B. et al., Harrison-Thompson Generalization of Bohm's Sheath Condition, Proc. Phys. Soc. **74** 145. (1959)

[10] KRYCHOWIAK M. et al., Overview of diagnostic performance and results for the first operation phase in Wendelstein 7-X, REVIEW OF SCIENTIFIC INSTRUMENTS **87** (2016) 11D304

[11] JAKUBOWSKI M. et al., Scrape-off layer physics in the initial campaign of Wendelstein 7-X, EPS Belfast 2017 I2.106

[12] BOZHENKOV S. et al., Service oriented architecture for scientific analysis at W7-X. An example of a field line tracer, Fusion Engineering and Design **88** (2013) 2997 3006

[13] AKERSON A.R. et al., Three-dimensional scrape off layer transport in the helically symmetric experiment HSX, Plasma Phys. Control. Fusion **58** (2016) 084002

[14] OHYABU N. et al., Edge Thermal Transport Barrier In LHD Discharges, Phys. Rev. Lett. **84** 103 (2000)

[15] EICH T. et al., Inter-ELM Power Decay Length for JET and ASDEX Upgrade: Measurement and Comparison with Heuristic Drift-Based Model, PRL. **107** (2011) 215001

[16] SUN H. J. et al., Study of near scrape-off layer (SOL) temperature and density gradient lengths with Thomson scattering, Plasma Phys. Control. Fusion **57** (2015) 125011

[17] KALLENBACH A. et al., Multi-machine comparisons of H-mode separatrix densities and edge profile behaviour in the ITPA SOL and Divertor Physics Topical Group, Journal of Nuclear Materials 337-339 (2005) 381-385

[18] BOZHENKOV S. et al., Limiter for the early operation phase of W7-X, Proceedings of the 41nd EPS, (2014)

[19] GADELMEIER F. et al., Conditions for island divertor operation in the W7-AS Stellarator, Proceedings of the 28nd EPS (2001)

[20] MASUZAKI S. et al., The divertor plasma characteristics in the Large Helical Device, Nucl. Fusion **42** (2002) 750758

[21] WURDEN G.A. et al, Limiter observations during W7-X first plasmas, Nucl. Fusion **57** (2017) 056036

[22] KRÄMER-FLECKEN A. et al., Investigation of turbulence rotation in limiter plasmas at W7-X with a new installed Poloidal Correlation Recflectrometry, Nucl. Fusion **57** (2017) 066023

[23] NIEMANN H. et al, Power loads in the limiter phase of Wendelstein 7-X, Proceedings of the 43nd EPS (2016) (http://ocs.ciemat.es/EPS2016PAP/pdf/P4.005.pdf)

[24] LIANG Y. et al., Diagnostic setup and modelling for investigation of synergy between 3D edge physics and plasma wall interactions on W7-X, Nucl. Fusion **57** (2017) 066049

Acknowledgements

The author would like to thank B. Stanley of the IPP Greifswald for setting up and explaining the data aquisition system at W7-X for the multi-purpose manipulator and P. Sinha and H. Niemann of the IPP Greifswald for helping with debugging the connection length calculation.

This work has been carried out within the framework of the EUROfusion Consortium and has received funding from the Euratom research and training programme 2014-2018 under grant agreement No 633053. The views and opinions expressed herein do not necessarily reflect those of the European Commission.